Stimulated emission due to spatially separated electron-hole plasma and exciton system in homoepitaxial GaN

K. Kazlauskas, G. Tamulaitis, and A. Žukauskas
Institute of Materials Science and Applied Research, Vilnius University, Saulėtekio 9-III, LT-10222 Vilnius, Lithuania

T. Suski, P. Perlin, M. Leszczynski, P. Prystawko, and I. Grzegory
UNIPRESS, High Pressure Research Center, Sokolowska 29, 01-142 Warszawa, Poland
(Received 29 October 2003; revised manuscript received 27 January 2004; published 24 June 2004)

Stimulated emission under quasi-resonant photoexcitation was studied in high-quality homoepitaxial GaN layers. Emission escaping perpendicular to the excited surface as well as propagating along the surface was analyzed as a function of the excitation power density in the temperature range from 8 to 600 K. Contributions of stimulated emission due to inelastic exciton–exciton/carrier interaction and recombination in electron-hole plasma (EHP) were revealed and simultaneously observed from the sample edge. The concurrent action of two mechanisms of stimulated emission was interpreted to be caused mainly by spatially inhomogeneous Mott transition due to separation of EHP located at the very surface of the layer and dense exciton gas located deeper in the layer. The separation is facilitated by high carrier diffusion length in homoepitaxial GaN. Stimulated emission due to inelastic exciton–exciton/carrier interaction was unambiguously traced up to the temperature of 440 K.

DOI: 10.1103/PhysRevB.69.245316 PACS number(s): 78.55.Cr, 71.35.Ee, 71.35.Gg, 78.45.+h

I. INTRODUCTION

Recently, InGaN/GaN quantum well based laser diodes (LDs) and light-emitting diodes (LEDs) became indispensable commercial solid-state light sources in the green/blue/violet spectral regions.[1,2] A rapid increase in the market potential of the LEDs is stimulated mainly by their applications in traffic lights, large scale full-color displays, LCD backlighting, and white sources of light, while the LDs have good prospective in high-density optical storage, high-resolution printing, and projection displays.[3,4] However, a large variety of important applications such as detection of biological and chemical agents, medical diagnostics, phototherapy, disinfection, deodorization, and solid-state lighting require efficient light sources in the UV spectral region.[5] Therefore, use of pure GaN or $Al_xGa_{1-x}N$ layers in the active region of UV emitters is highly desirable. In spite of such a great importance of GaN for its utilization in multilayered heterostructures for the green/blue/violet and UV light emitters, comprehensive understanding of the intrinsic emission processes in GaN is not unambiguously established so far.

Since GaN layers are usually grown by heteroepitaxy on sapphire or SiC substrates, they contain a very large density of threading dislocations ($\sim 10^8-10^{10}$ cm^{-2}) because of a large lattice and thermal mismatch with the substrate.[6,7] GaN layers with a high density of dislocations are not desirable for fabrication of advanced light-emitters, since dislocations serve as nonradiative centers for nonequilibrium carriers and deteriorate efficiency of light emission.[8–10] Also, dislocations were found to be a major cause of degradation of laser diodes, which operate at high current density.[11,12] Despite of enormous efforts to reduce the density of threading dislocations by employing low-temperature-interlayer technology[13] and epitaxial lateral overgrowth technique[14,15] with its numerous modifications,[16,17] typical dislocation density in GaN layers still remains high ($\sim 10^6-10^7$ cm^{-2}).

The most radical solution of the substrate problem is homoepitaxy of GaN layers on bulk GaN substrates with low dislocation density. Such bulk crystals grown from solutions of atomic nitrogen in liquid Ga at high N_2 pressure and high temperature[18–21] contain less than 10^2 dislocations per cm^2.[22] (Very recently a liquid phase epitaxy method in a Ca–Na mixed flux system was proposed for the growth of large size GaN single crystals with a dislocation density below 2×10^5 cm^{-2}.[23]) Among all the available approaches, homoepitaxy is the only one, which is capable to deliver GaN layers of superior structural and optical quality with extremely low dislocation density.[24] Despite small size and high production cost that prevent large-scale applications (visible LEDs), homoepitaxy over GaN monocrystals might be the technology of choice for specific applications like high-power LDs and deep-UV LEDs, where exceptional quality is the first priority.

On the other hand, GaN homoepitaxy provides a unique opportunity to study almost strainless GaN layers with especially low density of structural defects,[25] high carrier mobility,[26] and long carrier lifetime.[21] In particular, this approach based on almost intrinsic GaN allows one to get a deeper insight into the processes of stimulated emission in this material.

Numerous experimental and theoretical studies of optical gain in GaN and related materials (see e.g., Refs. 27–35) may be pointed out as an indication of high importance of better understanding of the processes of stimulated emission for development of UV LDs. However, by using a conventional variable-stripe-length excitation method,[36] measurable values of the optical gain coefficient are well below 10^4 cm^{-1},[28,37,38] a maximum value predicted in GaN for intrinsic mechanisms of stimulation.[30] Therefore, measurements of the optical gain coefficient provide with poor information on the origin of stimulated emission and extended

spectral investigations are to be performed. Also, a deeper understanding of the mechanisms of spontaneous and stimulated emission is desirable for better characterization of GaN, what is important for various applications, especially in devices operating at high density of nonequilibrium carriers.

Following the first observation of stimulated emission from optically pumped single-crystal needles of GaN at 2 K in 1971,[39] two processes were pointed out as the most probable origin of stimulated emission in GaN: (i) inelastic exciton–exciton/carrier scattering resulting in radiative recombination of the exciton colliding with another exciton[40] or electron(hole), and (ii) recombination in EHP, which occurs at high-density and/or high-temperature regime.[41]

The competition of these two optical gain mechanisms depends mainly on carrier density and temperature. Optical amplification due to inelastic exciton–exciton collisions was observed at 80 K (Ref. 42) and up to 120 K in GaN needle crystals,[29] up to 150 K in MOCVD-grown GaN layers on sapphire,[31] up to 220 K in MOCVD-grown GaN layers on SiC,[31,32] and up to 180 K in HVPE-grown bulk GaN crystals.[33,34] To the best of our knowledge, the highest temperature of stimulated recombination due to excitons (300 K) was reported in GaN/AlGaN separate confinement heterostructures grown on SiC,[35] whereas stimulated emission was observed in GaN at temperatures as high as 700 K.[31,43] Generally, the higher the temperature for exciton-related stimulated emission to manifest itself, the higher the quality of the crystal.

The present paper is aimed at the study of stimulated emission in homoepitaxial MOCVD-grown GaN with exclusively high structural quality[18] and long lifetime of nonequilibrium carriers.[21] We study emission propagating both perpendicular and parallel to the photoexcited surface of the crystal under excitation power densities within a large dynamic range and at temperatures ranging from 8 K to 600 K. By studying emission that emerges from the edge of the excited sample, we demonstrate stimulated emission under conditions of the inhomogeneous Mott transition that results mainly in spatial separation of electron-hole plasma located at the very surface of the crystal and dense exciton gas located deeper in the crystal. We conclude that in homoepitaxial GaN, stimulated emission due to inelastic exciton–exciton/carrier scattering can be observed up to temperatures as high as 440 K.

II. EXPERIMENT

MOCVD-grown homoepitaxial GaN layers of 1 μm thickness were deposited on hexagonal bulk GaN substrates prepared from solutions of atomic nitrogen in liquid Ga at high N_2 pressure and high temperature (high nitrogen pressure solution method, HNPS).[18] X-ray diffraction analysis of these layers revealed about 20 arcsec linewidth for the (0004) reflex using Cu-*K* alpha radiation.[19] Transmission electron microscopy, defect selective etching, and atomic force microscopy revealed a very low dislocation density in these layers (less than 10^2 dislocations per cm^2).[22]

As compared with heteroepitaxial GaN layers on sapphire grown at identical conditions, homoepitaxial layers under study exhibited extremely long carrier lifetimes at high excitation (890 ps in homoepitaxial and 190 ps in heteroepitaxial GaN layers at room temperature).[44] The long lifetime was attributed to a significantly lower density of nonradiative decay centers, and thus, to improved quality of homoepitaxial GaN layers. Moreover, lowering of the threshold for stimulated emission and considerable enhancement of optical gain at fixed excitation conditions were observed in the homoepitaxial layer, as compared to the heteroepitaxial layers.[44]

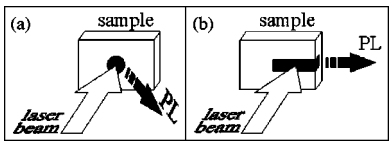

FIG. 1. Sample excitation geometries: front-surface (a) and lateral (b).

The homoepitaxial GaN samples under study were primarily characterized by measuring photoluminescence (PL) under low-power continuous-wave (cw) excitation by He–Cd laser operating at 325 nm wavelength. Quasi-steady-state PL experiments at excitation power densities of up to $\sim$10 MW/cm^2 were carried out by using a Q-switched Nd:YAG laser (pulse duration 10 ns). The frequency-tripled laser radiation (3.50 eV) served for band-to-band GaN excitation with small excess energy of the photoexcited carriers (quasi-resonant excitation). Use of quasiresonant photoexcitation was critical for resolving spectral bands, while a nonresonant photoexcitation with a high photon excess energy (4.66 eV) resulted in broadening and overlapping of PL bands due to carrier heating, as studied in more details for heteroepitaxial GaN.[45]

The PL signal was dispersed by a 0.6-m double monochromator (Jobin Yvon HRD 1) and detected by using a UV-enhanced photomultiplier tube (Hamamatsu R1463P). Single photon counting technique was used in the cw regime, while the spectra under pulsed excitation were recorded by a boxcar integrator. A closed-cycle helium refrigerator was utilized for cooling the samples down to 8 K and the measurements were carried out in the temperature range up to 600 K.

To distinguish between spontaneous and stimulated emission, PL spectra under pulsed excitation were measured in two configurations. The luminescence collected in front-surface configuration from an excited spot of 0.3 mm in diameter [see Fig. 1(a)] contained contribution mainly due to spontaneous emission. In lateral configuration, amplified light propagating along the sample surface was detected. The light was collected from the cleaved edge of the crystal in the direction along a 30-μm wide stripe focused on the crystal surface by using a cylindrical lens [see Fig. 1(b)]. The laser beam was directed perpendicularly to the front surface of the sample in both configurations.

It is worth noting that all PL data presented below refers to the epilayer, since the bulk GaN substrate exhibits low luminescence efficiency, probably, because of unintentional oxygen doping.[22]

III. RESULTS AND DISCUSSION

Figure 2 displays a PL spectrum of the homoepitaxial GaN layer measured at 8 K using a cw 0.1-W/cm^2 excita-

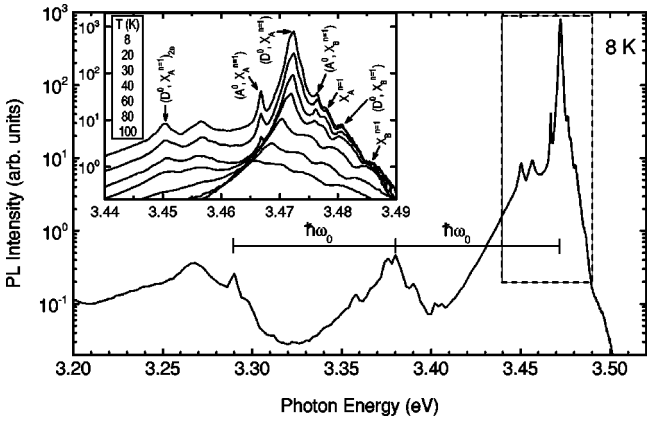

FIG. 2. Low-excitation PL spectrum measured in front-surface configuration at 8 K. $\hbar\omega_0$ is the longitudinal-optical phonon energy separating the first and the second replicas of the dominant $(D^0,X_A{}^{n=1})$ peak shown inside the dashed rectangle. The inset demonstrates the enlarged view of the spectrum in the dashed-rectangular area together with the PL spectra at different temperatures (indicated).

tion power density. The edge luminescence region is presented in more details at several temperatures in the inset. The spectrum is dominated by donor-bound exciton (D^0,X) emission. Acceptor-bound exciton (A^0,X) as well as free *A*- and *B*- exciton emission lines (indicated as $X_A{}^{n=1}$ and $X_B{}^{n=1}$, respectively) may also be identified as in Ref. 20. The line $(D_0,X_A{}^{n=1})$ peaked at 3.4720 eV is caused by recombination of donor-bound exciton with a hole from the *A* valence band. It is commonly believed that this line originates from Si and O donor impurities in undoped GaN grown by different techniques.[46] The width (~1.5 meV) and shape of the line shows that it probably consists of several closely stacked ~0.1-meV wide lines that were resolved in GaN layers grown on pretreated GaN single crystals.[47] Peaks due to free *A*-exciton emission at 3.4780 eV as well as free *B*-exciton emission at 3.4860 eV are resolved on the high-energy slope of the main line. The *A*-exciton binding energy to the neutral donor, D^0, determined from the energy separation (~6 meV) between the peaks $(D^0,X_A{}^{n=1})$ and $X_A{}^{n=1}$ is consistent with that of Ref. 47. Separation of the line peaked at 3.4805 eV from the *B*-exciton peak is also ~6 meV, thus the line can be attributed to *B* exciton bound to the same neutral donor $(D^0,X_B{}^{n=1})$. The PL peak at 3.4665 eV with FWHM of ~0.7 meV is attributed to an *A*-exciton bound to shallow acceptor $(A^0,X_A{}^{n=1})$. The peak position is within 1-meV agreement with that in Ref. 47. Recombination of *B* exciton bound to the same neutral acceptor, A_0, results in the line $(A^0,X_B{}^{n=1})$ peaked at 3.4765 eV. The so called two-electron transition $(D^0,X_A{}^{n=1})_{2e}$ involving radiative recombination of one electron with a hole leaving the neutral donor with the second electron in an excited state[47] was observed at ~3.450 eV. The peak at ~3.456 eV (without a label) might be associated with certain acceptor-bound exciton.[48] The small peak at ~3.498 eV is possibly related to free *C*-exciton emission. Most of the sharp peaks have replicas due to recombination assisted by emission of one or two longitudinal-optical (LO) phonons with the energy of $\hbar\omega_0$ =92.2 meV.[49]

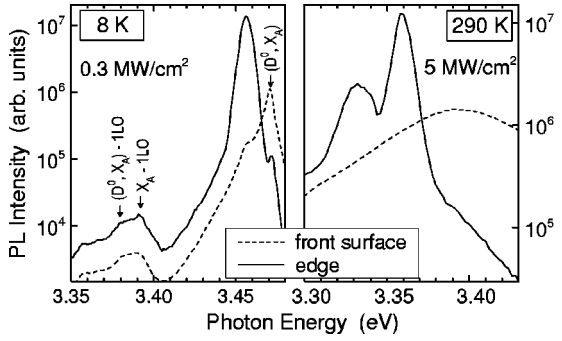

FIG. 3. Photoluminescence spectra of homoepitaxial GaN recorded at 8 and 290 K in front-surface (dashed line) and lateral (solid line) configurations. The excitation power densities and temperatures are indicated.

No substantial changes in the spectrum at low temperatures are detected with an increase of excitation power density by more than 5 orders of magnitude up to 10 kW/cm^2. The further increase of the pump density causes a considerable broadening and overlap of the lines, although the dominant donor-bound exciton peak might be resolved up to the highest pump densities. At room temperature and elevated pump densities, the luminescence spectrum consists of one broad feature caused by band-to-band transitions (see Fig. 3).

Essentially different spectra are observed in lateral configuration. Typical spectra in both configurations are compared in Fig. 3. Note the new bands that appear in lateral configuration but are not observed from the front surface of the sample.

Evolution of the lateral luminescence spectra with increasing the excitation power density is demonstrated in Fig. 4. At low temperatures and low pumping levels, the spectra are dominated by sharp lines originated from donor- and acceptor-bound excitons. An increase of the pump density results in a new narrow band peaked at 3.46 eV. The pump-density dependences of the PL intensity in the lateral and front-surface configurations are compared in Fig. 5. Data

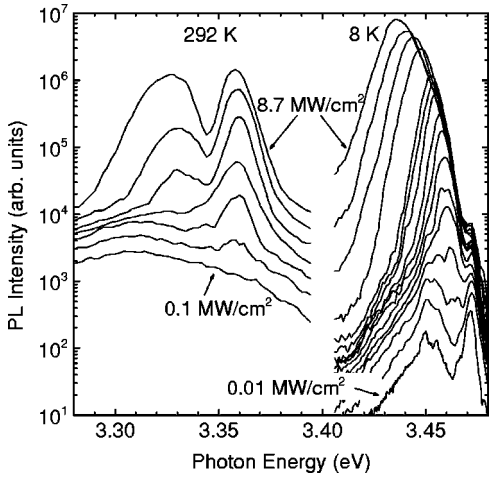

FIG. 4. Excitation power density dependence of the PL spectra measured in lateral configuration at 8 and 292 K. The pump density for each spectra depicted was increased incrementally by a factor of ~1.45.

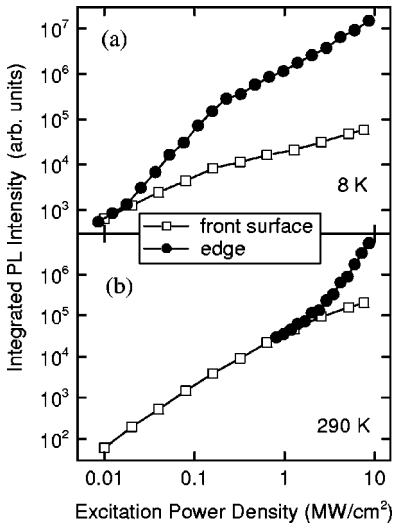

FIG. 5. Spectrally integrated PL intensity as a function of the excitation power density at 8 K (a) and 290 K (b) in front-surface (solid circles) and lateral (open squares) configurations, respectively. For comparison, the curves are collated by an arbitrary vertical shifting.

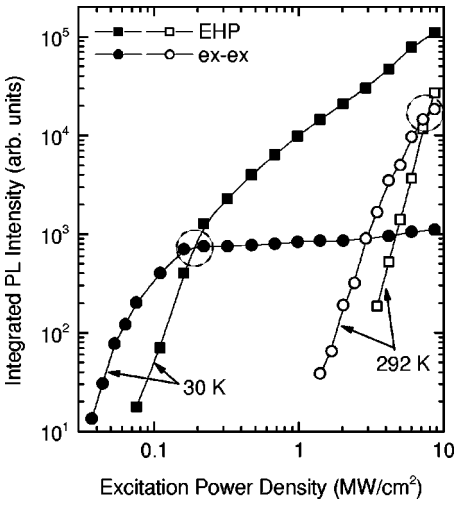

FIG. 6. Integrated PL intensity of stimulated emission bands as a function of the pump power density at two temperatures (indicated). Squares, the lower-energy stimulated band; circles, the higher-energy stimulated emission band. The crossovers of the each two curves are accentuated by dashed circles.

shown by points in Fig. 5 were obtained by integrating of the lateral PL spectra depicted in Fig. 4 and spontaneous PL spectra measured in front-surface configuration (not shown here) at each pump density. (A shift along the vertical axis is introduced in order to compare these dependencies.) Below a certain threshold, both the lateral and front-surface PL intensity exhibit almost linear dependencies on the pump density. Whereas above the threshold, the dependence for lateral configuration changes to a superlinear one providing with a clear evidence on an onset of stimulated emission. Note that at moderate excitation densities, the stimulated band maintains a constant linewidth and almost constant peak position. At the highest pump densities, the band broadens and redshifts rapidly.

Increased temperature results in thermal dissociation of bound excitons and, consequently, the sharp lines are no longer observed in the PL spectra at elevated temperatures (see spectra at 292 K in Fig. 4). Instead of sharp spectral features, a broad band due to partially reabsorbed spontaneous emission dominates the lateral PL spectra up to the pump power densities of $\sim 0.1\,\mathrm{MW/cm^2}$ with no substantial changes in the band shape. An increase in pump density gives rise to a band narrowing, i.e., a new emission band emerges on the high-energy slope of the reabsorbed spontaneous-luminescence band at 3.36 eV. The width and peak position of this new band show no considerable dependence on pump density in the same manner as the width and peak position of the stimulated emission band peaked at 3.46 eV do under moderate pump densities at 8 K.

However, the most striking feature of the dynamics of the spectra with increasing pump density at 292 K is a rapid emergence of the second band that is located at lower energies (3.33 eV at the threshold) with respect to the first band. In contrast to the first band, the second one drastically broadens and redshifts with pump density. Moreover, the evolution of the second band with increasing pump density is similar to that observed at 8 K for the highest pump densities. Note that at 292 K, the integrated PL intensity of the both bands peaking at 3.33 eV and 3.36 eV, respectively, also exhibits a superlinear increase versus excitation power density, as shown by solid circles in Fig. 5(b). Thus, the pump dynamics of the PL spectrum measured at 8 K and 292 K is similar, except that the two bands of the stimulated origin are easy to spectrally resolve at 292 K while they are strongly overlapped at 8 K. To verify the identical origin of these bands, a PL spectrum dependence on the pump density was measured by gradually increasing temperature from 8 K to 292 K. The measurements revealed that increased temperature facilitates resolving of the two stimulated emission bands. This is a surprising effect, since usually increased temperature facilitates an overlap of spectral lines due to thermal broadening.

To clarify such a contradictory temperature behavior of the two bands, the integrated PL intensity of each band was investigated separately as a function of pump density (see Fig. 6). The intensities of the overlapped bands were deduced by decomposition assuming that the width and peak position of the higher-energy band negligibly depends on pump density as it does at 292 K.

Figure 6 demonstrates that an increase of the pump density at 30 K is accompanied by a superlinear increase in the PL intensity of both stimulated emission bands up to the crossover of their intensities (indicated by a dashed circle). A further increase of the excitation density results in a boost of the intensity of the lower-energy stimulated band (indicated by solid squares) with respect to the higher-energy band (indicated by solid circles). In contrast, the intensity of the higher-energy band saturates just above the crossover and maintains a constant value up to the highest pump densities. A qualitatively similar evolution of the PL intensity of both stimulated emission bands with increasing the pump density up to the intensity crossover point is observed also at 292 K (see open points in Fig. 6). Due to the increased threshold of stimulated emission at 292 K, these dependencies, as well as

their crossover point are shifted towards a higher excitation density by more than one order of magnitude in respect to that observed at 30 K. At 292 K, the crossover is achieved at the highest pump density used in our experiment, and therefore, further saturation of the PL intensity of the higher-energy band, as was observed at lower temperatures, could not be attained. Note that at the highest pump density, the lower-energy stimulated-emission band is by two orders of magnitude more intense than that of the higher-energy band at 30 K, whereas the intensities of the two bands are very similar at 292 K. At 30 K, such a huge difference in intensity results in a strong overlap of the high-energy band by the much more intense lower-energy band. Given that at the highest pump density the separation between these bands is almost the same for all temperatures, this in part accounts for the overlap of the two bands at low temperatures.

The temperature and excitation power dynamics of lateral PL described above can reveal mechanisms of stimulated emission in homoepitaxial GaN. Basically, the intrinsic mechanisms of stimulated emission in semiconductors are related with excitons and EHP. Based on the almost constant linewidth and peak position versus excitation power density of the higher-energy lower-threshold stimulated emission band, it is reasonable to attribute this band either to inelastic exciton–exciton and/or exciton–carrier collisions. On the other hand, the rapid broadening and a strong red shift with an increase of the pump density of the lower-energy higher-threshold stimulated emission band is a well-known feature of the recombination in a dense free-carrier system.[50] Therefore, this band is probably due to EHP recombination.

To support the aforementioned assignments, the temperature and excitation power density dynamics of observed stimulated emission should be discussed in more detail. In particular, the PL intensity dependence on pump density of the two bands shown in Fig. 6 is consistent with a phase transition in the excitonic system. At 30 K, the boost of the stimulated emission intensity assigned to EHP in respect to the intensity of the exciton-related band can be attributed to the Mott transition. Increased carrier density completely screens Coulomb interaction between electrons and holes as soon as the critical density is reached. This results in a saturation of the intensity of the exciton-related band. Roughly, the crossover of intensities of the two bands, accentuated by a dashed circle in Fig. 6, indicates the Mott transition point.

As one can see in Fig. 6, a considerably higher pump density is required to achieve the Mott transition at elevated temperatures. In particular, for a temperature increase from 30 K to 292 K, an increase of the excitation power by a factor of about 40 is required to attain the crossover between the intensities of the exciton-related and plasma bands. We suggest that this effect is due to two reasons. First, the critical carrier density for the Mott transition increases with temperature. Generally, the Mott density can be deduced from an equation

$$a_B \kappa(n) = 1.19, \tag{1}$$

where a_B is an exciton Bohr radius and the square of the inverse screening length is

$$\kappa^2(n) = \frac{e^2 n}{\varepsilon_0 \varepsilon k_B T} \sum_{i=e,h} F_{-1/2}(\mu_i)/F_{1/2}(\mu_i). \tag{2}$$

Here, ε is the static permittivity, and $F_j(\mu_i)$ is a Fermi integral of the j order as a function of the reduced Fermi quasi-level μ_i, which is determined by the Mott density and temperature. For GaN, the Mott density calculated using Eq. (1) should increase by one order of magnitude when the temperature increases from 30 K to 292 K.

Second, a higher excitation density for achieving the Mott transition at higher temperatures might be required because of some temperature-induced decrease in carrier lifetime (in the same samples, the lifetime of the A exciton of 2.7 ns have been reported at low temperature[51] in contrast to 0.89-ns carrier lifetime at room temperature[44]). This can result in an additional half an order of magnitude for the crossover excitation power density at room temperature. The estimates presented can account for the observed temperature dynamics of the Mott transition.

Note that in the entire temperature range, stimulated emission in EHP occurs at photon energies lower than those for inelastic exciton–exciton/carrier collisions. This means that EHP attains the density required for the stimulation threshold only after the Mott transition, which is a result of band gap shrinkage below the exciton ground energy, i.e., of disappearance of excitons. Surprisingly, we observe both the exciton-related band and the EHP band simultaneously.

The simultaneous coexistence of stimulated emission due to two mechanisms, radiative exciton–exciton interaction and recombination of free carriers, was reported for GaN grown on SiC up to 220 K.[32] Formerly, such a coexistence in CdS and ZnO was attributed to phase separation within the excited area what results in a region filled with EHP and a region still exhibiting excitonic properties as confirmed by reflectivity and optical gain measurements using the two-beam as well as the variable-stripe-length methods.[52] Two overlapped stimulated-emission bands at low temperature were also distinguished by their different time behavior in CdS (Ref. 53) and interpreted by spatial separation of EHP and dense exciton system due to the decrease of the density of photoexcited carriers from crystal surface into its bulk (the inhomogeneous Mott transition).

Generally, the dual structure of an emission spectrum can be caused by both temporal and spatial inhomogeneity of the photoexcited carrier system. Under high excitation, EHP can be formed in regions with a higher carrier density, whereas excitons can reside in regions with a lower carrier density. In our case, spatial inhomogeneity should result from the transversal (almost Gaussian) profile of the excitation stripe and from the exponential depth profile of the carrier density due to diffusion perpendicularly to the surface of the sample. The diffusion-related profile can be even more flat (hyperbolic), where bimolecular recombination dominates. The temporal inhomogeneity results from the leading and trailing edges of the Gaussian excitation pulse (here, the pulse is long enough to assume that the carrier density follows the pulse shape). Since a Gaussian function has a much steeper decay than the exponential one (and even a much more steeper decay than the hyperbolic one), we conclude that the diffusion into the

bulk of the layer contributes to the emission from lower-density carrier system to a larger extent than the transverse spatial profile and the temporal tails do. Therefore at sufficiently high excitation densities, EHP should emit from the region at the very surface of the crystal, while the high-density excitonic system should contribute to the emission due mainly to the lower-density region located deeper in the crystal. The excitonic layer persists with increasing the excitation density, being "pushed" deeper and deeper into the crystal, however. We suppose that in homoepitaxial GaN, observation of spatial separation of two stimulated-emission bands in the lateral spectra up to temperature of 440 K is facilitated by a large length of carrier/exciton diffusion that results in spatial distribution of carriers and excitons on a relatively large depth, which considerably exceeds the penetration depth of the excitation light. As a result, an exciton system with a density high enough for stimulated emission can form a layer thick enough for the emission to be observed in lateral configuration. Our assumption on the negligible influence of the Gaussian tails (both spatial and temporal) is supported by the fact that in front-surface configuration, only one spontaneous-recombination band is observed, probably due to EHP, whereas spontaneous emission due to exciton–exciton/carrier collisions is strongly reabsorbed in the surface layer.

Note that the absence of stimulated emission in the front-surface configuration also indicates high structural quality and a low density of cracks in the homoepitaxial GaN, since cracks and rough surface are known to scatter stimulated emission propagating along the surface of the photoexcited crystal.[54]

The diffusion-related spatially inhomogeneous Mott transition is capable of accounting for simultaneous observation of two stimulated-emission bands. To give a reasonable explanation of the "anomalous" spectral separation of these bands with increasing temperature, band gap renormalization at the threshold of stimulated emission in EHP should be considered. According to Ref. 55, the change in the band gap energy due to renormalization (above the Mott density) is

$$\delta E_g = -\frac{E_R \pi^2 a_B}{12}\kappa, \tag{3}$$

where E_R is the exciton Rydberg.

In order to compare the influence of band gap renormalization at the stimulation threshold for 30 K and 292 K, the threshold carrier density, n_0, should be estimated at each temperature. By utilizing the condition of the onset of free-carrier gain, i.e., the transparency point,[56] $\mu_e+\mu_h \approx E_g$, we estimate the threshold carrier density for GaN to be $n_0(30\ \mathrm{K}) \cong 1.4\times 10^{17}\ \mathrm{cm}^{-3}$ and $n_0(292\ \mathrm{K}) \cong 4.2 \times 10^{18}\ \mathrm{cm}^{-3}$. These calculations yield a factor of ~ 1.8 for the ratio $\delta E_g(292\ \mathrm{K})/\delta E_g(30\ \mathrm{K})$. This means that at low temperature, the onset of stimulated emission due to EHP occurs at smaller band gap renormalization than that at high temperature. Meanwhile, the exciton energy is known to be almost insensitive to the carrier density. As a consequence, in the vicinity of the Mott transition the exciton-related and the EHP bands are stronger overlapped at 30 K, whereas they

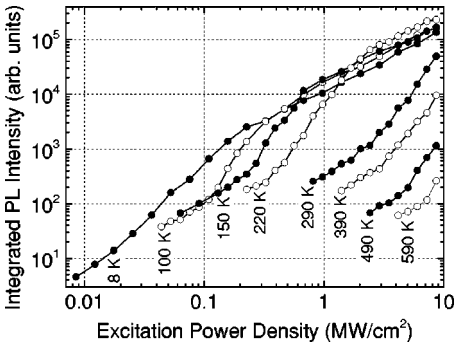

FIG. 7. Integrated PL intensity as a function of excitation power density at various temperatures (indicated).

can be clearly resolved at 292 K. Note, that the pump densities at the stimulation threshold of EHP (see Fig. 6) are consistent with the ratio $n_0(30\ \mathrm{K})/n_0(292\ \mathrm{K})$ with the aforementioned temperature-induced decrease of the carrier lifetime taken into account.

Our results clearly indicate that in homoepitaxial GaN epilayers, the threshold of stimulated emission at room temperature is predetermined by inelastic exciton–exciton/carrier collisions in partially ionized exciton gas. (The excitonic origin of stimulated emission is expected to manifest itself even stronger in relevant quantum structures, which may offer enhanced exciton binding energy.) To set the temperature limits for exciton-related stimulated emission in homoepitaxial GaN, which to our opinion is the most close to intrinsic crystal, we have measured the lateral PL spectra up to 600 K. The dependence of the integrated PL intensity versus the excitation power density at various temperatures is illustrated in Fig. 7, whereas the spectral dynamics with increasing temperature is shown in Fig. 8.

As can be seen in Fig. 7, the threshold behavior of stimulated emission (a crossover from a linear to superlinear dependence of the lateral PL intensity versus pump density with the front-surface PL intensity keeping almost linear dependence) can be resolved up to the temperature of 590 K. The superlinear lateral PL intensity versus pump density dependence tends to saturate at the highest pump densities. Such a saturation is a typical feature of stimulated emission and is caused by depletion of population inversion due to amplified emission propagating in the inverted medium, provided that the gain is high enough.[36] With increased temperature, the saturation point is seen to shift to higher excitation densities. Above 290 K, the saturation cannot be attained even at the highest pump used (see Fig. 7) indicating that stimulated emission is no more able to dominate recombination, probably, because of an increased role of nonradiative capture.

Figure 8 displays the spectra of lateral PL measured at two pump densities for each of the given temperatures. Dashed curves indicate the lateral PL spectra measured at the highest pump density ($8.7\ \mathrm{MW/cm^2}$). Solid curves display the spectra of lateral PL measured at pump densities most favorable for the observation of the high-energy stimulated emission band. To reveal the peak shift, the spectra are normalized. The temperature behavior of the lateral emission spectra indicates that starting with about 200 K, two

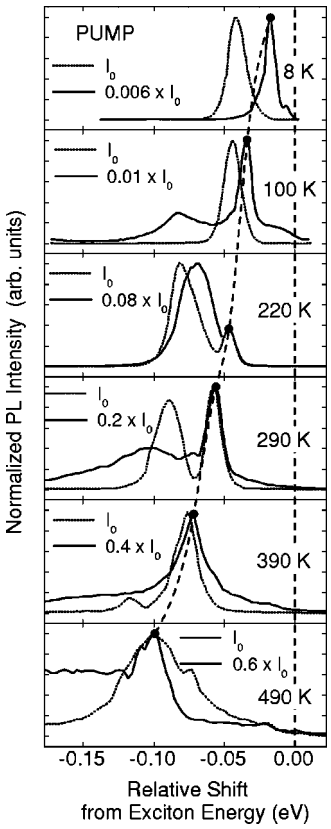

FIG. 8. PL spectra measured at two pump intensities in lateral configuration ($I_0 = 8.7$ MW/cm^2) for different temperatures (indicated). The energy axis of each spectrum is presented as relative to the exciton energy indicated by the vertical dashed line. The dashed curve connecting the peaks is a guideline for the eye.

stimulated-emission bands can be resolved. The lower-energy band, which is obviously due to EHP, can still be resolved at 390 K (see Fig. 9) and it completely disappears at 440 K. The exciton-related higher-energy band, which exhibits an almost constant peak position and linewidth, persists even for higher temperatures. However because of absence of double structure of the spectra, we unambiguously set the high-temperature limit for manifestation of excitons in stimulated emission from GaN to at least 440 K. (To the best of our knowledge, the stimulated emission due to radiative exciton-exciton/carrier interaction has not been observed in GaN at such high temperatures.) Above 440 K, only one broad feature descending from the higher-energy band is observed in the stimulated-emission spectra with an excitonic contribution still being possible.

To provide with additional evidence on the significant contribution of the inelastic exciton–exciton/carrier scattering to stimulated emission in a wide range of temperatures, we collated the temperature dependence of the peak energy of the stimulated emission bands with numerical calculations of the gain spectrum due to stimulated exciton–exciton and exciton–carrier recombination (exciton–LO phonon interactions was also considered). Points in Fig. 9 represent the experimental peak positions of the stimulated-emission bands that were attributed to inelastic exciton–exciton/carrier interaction (solid points) and recombination in EHP (open triangles), respectively. Since the peak positions depend not only on temperature but also on the pump density, we selected the points that correspond to the highest pump densities applied.

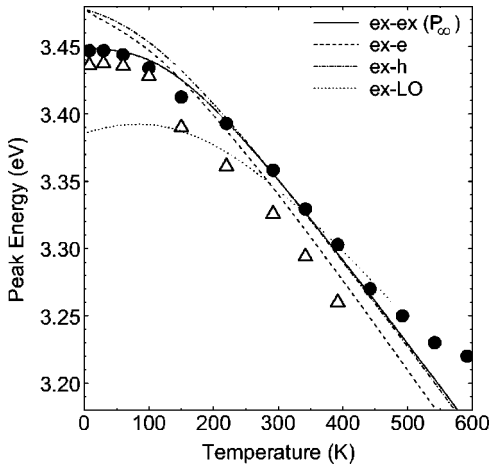

FIG. 9. Temperature dependence of the peak energy of the stimulated emission bands due to exciton-related phenomena (solid points) and EHP (open triangles) at the highest pump density of 8.7 MW/cm^2, respectively. Lines represent results of numerical modeling of inelastic exciton–exciton (P_∞ band, solid line), exciton–electron (dashed line), exciton–hole (dashed–dotted line), and exciton–LO phonon (dotted line) scattering for exciton density at the Mott transition.

The numerical calculations were performed by taking into account Coulomb and exchange interactions between an electron and hole as introduced by Moriya and Kushida[57,58] (for exciton–exciton interaction) and Benoit à La Guillaume[59] (for exciton–carrier and exciton–LO phonon interaction). Polariton effects were also taken into account by incorporating a term containing the exciton polarizability, the value of which for the homoepitaxial GaN was taken from the Ref. 60. The temperature-induced band gap shrinkage was introduced by using the temperature-dependent exciton energy described by a Bose-Einstein–type expression $E_0^{1S}(T) = E_0^{1S}(0) - \lambda/\exp(\beta/T - 1)$, where the values of 3.478 eV, 0.121 eV, and 316 K were taken for the exciton energy at zero temperature $E_0^{1S}(0)$ and the coefficients λ and β, respectively.[61] The highest possible exciton density, i.e., the Mott density, was used in calculations at each temperature point.

The dependencies depicted by lines in Fig. 9 represent the peak energy of the calculated optical gain spectra. A fairly good agreement between the calculated and experimental data evidences that at low temperature (up to $\sim$150 K), inelastic exciton–exciton collisions with one of the interacting excitons scattered to the exciton continuum dominate stimulated emission. At higher temperatures, several exciton related processes, such as exciton–exciton and/or exciton–carrier collisions can contribute stimulated emission. These mechanisms are difficult to distinguish because of their similar temperature dependence of the peak energy above 150 K. In addition above 300 K, exciton–LO phonon should not be excluded as well. Above 500 K, the mechanism of stimulated emission is difficult to identify because of lack of experimental data above the threshold of stimulation.

IV. CONCLUSIONS

To summarize, photoluminescence emitted from the front surface and emission propagating along the sample surface was studied as a function of temperature and excitation power density in homoepitaxial GaN under quasiresonant quasi-steady-state excitation conditions. The results of the study evidence that light is mainly amplified by two mechanisms, namely recombination in EHP and inelastic exciton–exciton/carrier collisions. In a certain range of excitation densities and temperatures, the bands of stimulated emission due to these two processes are simultaneously observed. This concurrent stimulated emission of different origin is consistent with a model of the spatially inhomogeneous Mott transition due mainly to separation of EHP located at the sample surface and the dense exciton system located deeper from the surface. High structural quality and high carrier lifetime in homoepitaxial GaN ensures large diffusion length of the photoexcited excitons, and, consequently, a large thickness of the layer containing excitons at a density high enough for stimulated emission to occur. Stimulated emission due to inelastic exciton–exciton/carrier collisions was unambiguously traced up to a remarkably high temperature of ~440 K. These results show a high potential of homoepitaxial GaN in UV optoelectronics and might be utilized to identify mechanisms of the stimulated emission in GaN layers of different quality.

ACKNOWLEDGMENTS

The research at Vilnius University was partially supported by the Lithuanian State Science and Education Foundation and European Commission supported SELITEC center Contract No.G5MA-CT-2002-04047. A. Ž. acknowledges the Lithuanian Ministry of Education and Science for financial support. The research in Warsaw was partially supported by State Committee for Scientific Research (Poland), Project No. 2700/C.T11-8/2000.

[1] S. Nakamura, Semicond. Sci. Technol. **14**, R27 (1999).
[2] S. Nakamura, Solid State Commun. **102**, 237 (1997).
[3] S. Nakamura and G. Fasol, *The Blue Laser Diode: GaN Based Light Emitters and Lasers* (Springer-Verlag, Berlin, 1997).
[4] F. A. Ponce and D. P. Bour, Nature (London) **386**, 351 (1997).
[5] A. Žukauskas, M. S. Shur, and R. Gaska, *Introduction to Solid-State Lighting* (Wiley, New York, 2002).
[6] D. Kapolnek, X. H. Wu, B. Heying, S. Keller, B. P. Keller, U. K. Mishra, S. P. DenBaars, and J. S. Speck, Appl. Phys. Lett. **67**, 1541 (1995).
[7] F. A. Ponce, B. S. Krusor, J. S. Major, W. E. Plano, and D. F. Welch, Appl. Phys. Lett. **67**, 410 (1995).
[8] S. J. Rosner, E. C. Carr, M. J. Ludowise, G. Girolami, and H. I. Erikson, Appl. Phys. Lett. **70**, 420 (1997).
[9] T. Sugahara, H. Sato, M. S. Hao, Y. Naoi, S. Kurai, S. Tottori, K. Yamashita, K. Nishino, L. T. Romano, and S. Sakai, Jpn. J. Appl. Phys., Part 2 **37**, L398 (1998).
[10] T. Hino, S. Tomiya, T. Miyajima, K. Yanashima, S. Hashimoto, and M. Ikeda, Appl. Phys. Lett. **76**, 3421 (2000).
[11] S. Nakamura, Science **281**, 956 (1998).
[12] S. Nagahama, N. Iwasa, M. Senoh, T. Matsushita, Y. Sugimoto, H. Kiyoku, T. Kozaki, M. Sano, H. Matsumura, H. Umemoto, K. Chocho, and T. Mukai, Jpn. J. Appl. Phys., Part 2 **39**, L647 (2000).
[13] M. Iwaya, T. Takeuchi, S. Yamaguchi, C. Wetzel, H. Amano, and I. Akasaki, Jpn. J. Appl. Phys., Part 2 **37**, L316 (1998).
[14] A. Usui, H. Sunakawa, A. Sakai, and A. A. Yamaguchi, Jpn. J. Appl. Phys., Part 2 **36**, L899 (1997).
[15] P. Vennegues, B. Beaumont, V. Bousquet, M. Vaille, and P. Gibart, J. Appl. Phys. **87**, 4175 (2000).
[16] I. Kidoguchi, A. Ishibashi, G. Sugahara, and Y. Ban, Appl. Phys. Lett. **76**, 3768 (2000).
[17] T. S. Zheleva, S. A. Smith, D. B. Thomson, K. J. Linthicum, P. Rajagopal, and R. F. Davis, J. Electron. Mater. **28**, L5 (1999).
[18] S. Porowski, I. Grzegory, and J. Jun, in *High Pressure Chemical Synthesis*, edited by J. Jurczak, and B. Baranowski (Elsevier, Amsterdam, 1989), p. 21.
[19] C. Kirchner, V. Schwegler, F. Eberhard, M. Kamp, K. J. Ebeling, K. Kornitzer, T. Ebner, K. Thonke, R. Sauer, P. Prystawko, M. Leszczynski, I. Grzegory, and S. Porowski, Appl. Phys. Lett. **75**, 1098 (1999).
[20] M. Leszczynski, B. Beaumont, E. Frayssinet, W. Knap, P. Prystawko, T. Suski, I. Grzegory, and S. Porowski, Appl. Phys. Lett. **75**, 1276 (1999).
[21] S. Juršėnas, N. Kurilčik, G. Kurilčik, A. Žukauskas, P. Prystawko, M. Leszczynski, T. Suski, P. Perlin, I. Grzegory, and S. Porowski, Appl. Phys. Lett. **78**, 3776 (2001).
[22] I. Grzegory, Acta Phys. Pol. A **98**, 183 (2000).
[23] F. Kawamura, T. Iwahashi, M. Morishita, K. Omae, M. Yoshimura, Y. Mori, and T. Sasaki, Jpn. J. Appl. Phys., Part 2 **42**, L4 (2003).
[24] I. Grzegory and S. Porowski, Thin Solid Films **367**, 281 (2000).
[25] M. Leszczynski, H. Teisseyre, T. Suski, I. Grzegory, M. Bockowski, J. Jun, S. Porowski, K. Pakula, J. M. Baranowski, C. T. Foxon, and T. S. Cheng, Appl. Phys. Lett. **69**, 73 (1996).
[26] E. Frayssinet, W. Knap, P. Lorenzini, N. Grandjean, J. Massies, C. Skierbiszewski, T. Suski, I. Grzegory, S. Porowski, G. Simin, X. Hu, M. A. Khan, M. S. Shur, R. Gaska, and D. Maude, Appl. Phys. Lett. **77**, 2551 (2000).
[27] W. W. Chow, A. Knorr, and S. W. Koch, Appl. Phys. Lett. **67**, 754 (1995).
[28] G. Frankowsky, F. Steuber, V. Harle, F. Scholz, and A. Hangleiter, Appl. Phys. Lett. **68**, 3746 (1996).
[29] R. Cingolani, M. Ferrara, and M. Lugara, Solid State Commun. **60**, 705 (1986).
[30] K. Domen, K. Kondo, A. Kuramata, and T. Tanahashi, Appl. Phys. Lett. **69**, 94 (1996).
[31] S. Bidnyk, T. J. Schmidt, B. D. Little, and J. J. Song, Appl. Phys. Lett. **74**, 1 (1999).
[32] J.-C. Holst, L. Eckey, A. Hoffmann, I. Broser, H. Amano, and I. Akasaki, MRS Internet J. Nitride Semicond. Res. **2**, 25 (1997).
[33] L. Eckey, J.-C. Holst, A. Hoffmann, I. Broser, T. Detchprom, and

K. Hiramatsu, MRS Internet J. Nitride Semicond. Res. **2**, 1 (1997).
[34] W. D. Herzog, G. E. Bunea, M. S. Unlu, B. B. Goldberg, and R. J. Molnar, Appl. Phys. Lett. **77**, 4145 (2000).
[35] S. Bidnyk, J. B. Lam, B. D. Little, Y. H. Kwon, J. J Song, G. E. Bulman, H. S. Kong, and T. J. Schmidt, Appl. Phys. Lett. **75**, 3905 (1999).
[36] K. L. Shaklee, R. E. Nahory, and R. F. Leheny, J. Lumin. **7**, 284 (1973).
[37] S. T. Kim, H. Amano, I. Akasaki, and N. Koide, Appl. Phys. Lett. **64**, 1535 (1994).
[38] S. Hess, R. A. Taylor, J. F. Ryan, B. Beaumont, and P. Gibart, Appl. Phys. Lett. **73**, 199 (1998).
[39] R. Dingle, K. L. Shaklee, R. F. Leheny, and R. B. Zetterstrom, Appl. Phys. Lett. **19**, 5 (1971).
[40] J. M. Hvam and E. Ejder, J. Lumin. **12/13**, 611 (1976).
[41] R. Dai, W. Zhuang, K. Bohnert, and C. Klingshirn, Z. Phys. B: Condens. Matter **46**, 189 (1982).
[42] I. M. Catalano, A. Cingolani, M. Ferrara, M. Lugara, and A. Minafra, Solid State Commun. **25**, 349 (1978).
[43] S. Bidnyk, B. D. Little, T. J. Schmidt, Y. H. Cho, J. Krasinski, J. J. Song, B. Goldenberg, W. Yang, W. G. Perry, M. D. Bremser, and R. F. Davis, J. Appl. Phys. **85**, 1792 (1999).
[44] S. Juršėnas, G. Kurilčik, N. Kurilčik, G. Tamulaitis, K. Kazlauskas, A. Žukauskas, P. Prystawko, M. Leszczynski, T. Suski, P. Perlin, I. Grzegory, and S. Porowski, Proc. SPIE **123**, 4318 (2001).
[45] S. Juršėnas, G. Kurilčik, G. Tamulaitis, A. Žukauskas, R. Gaska, M. S. Shur, M. A. Khan, and J. W. Yang, Appl. Phys. Lett. **76**, 2388 (2000).
[46] B. Monemar, J. Mater. Sci.: Mater. Electron. **10**, 227 (1999).
[47] K. Kornitzer, M. Grehl, K. Thonke, R. Sauer, C. Kirchner, V. Schwegler, M. Kamp, M. Leszczynski, I. Grzegory, and S. Porowski, Physica B **273-274**, 66 (1999).
[48] V. Kirilyuk, A. R. A. Zauner, P. C. M. Christianen, J. L. Weyher, P. R. Hageman, and P. K. Larsen, Appl. Phys. Lett. **76**, 2355 (2000).
[49] M. E. Levinshtein, S. L. Rumyantsev, and M. S. Shur, *Properties of Advanced Semiconductor Materials: GaN, AlN, InN, BN, SiC, and SiGe* (Wiley, New York, 2001).
[50] C. F. Klingshirn, *Semiconductor Optics* (Springer-Verlag, Berlin, 1997).
[51] T. Taliercio, M. Gallart, P. Lefebvre, A. Morel, B. Gil, J. Allèegre, N. Grandejan, J. Massies, I. Grzegory, and S. Porowski, Solid State Commun. **117**, 445 (2001).
[52] K. Bohnert, G. Schmieder, and C. Klingshirn, Phys. Status Solidi B **98**, 175 (1980).
[53] H. Saito and E. O. Göbel, Phys. Rev. B **31**, 2360 (1985).
[54] S. Bidnyk, T. J. Schmidt, G. H. Park, and J. J. Song, Appl. Phys. Lett. **71**, 729 (1997).
[55] L. Bányai and S. W. Koch, Z. Phys. B: Condens. Matter **63**, 283 (1986).
[56] W. W. Chow and S. W. Koch, *Semiconductor-Laser Fundamentals* (Springer-Verlag, Berlin, 1999).
[57] T. Moriya and T. Kushida, J. Phys. Soc. Jpn. **40**, 1668 (1976).
[58] T. Moriya and T. Kushida, J. Phys. Soc. Jpn. **40**, 1676 (1976).
[59] C. Benoit à La Guillaume, J.-M. Debever, and F. Salvan, Phys. Rev. **177**, 567 (1969).
[60] R. Stepniewski, K. P. Korona, A. Wysmolek, J. M. Baranowski, K. Pakula, M. Potemski, G. Martinez, I. Grzegory, and S. Porowski, Phys. Rev. B **56**, 15151 (1997).
[61] K. P. Korona, A. Wysmolek, K. Pakula, R. Stepniewski, J. M. Baranowski, I. Grzegory, B. Lucznik, M. Wroblewski, and S. Porowski, Appl. Phys. Lett. **69**, 788 (1996).